Mathematical Modelling and Control

http://www.aimspress.com/journal/mmc

MMC, 4(1): 17–31.
DOI: 10.3934/mmc.2024003
Received: 18 June 2023
Revised: 04 December 2023
Accepted: 15 December 2023
Published: 15 March 2024

Research article

Synchronization for discrete coupled fuzzy neural networks with uncertain information via observer-based impulsive control

Weisong Zhou[1,*], **Kaihe Wang**[1] **and Wei Zhu**[2]

[1] College of Science, Chongqing University of Posts and Telecommunications, Chongqing 400065, China

[2] Key Laboratory of Intelligent Analysis and Decision on Complex Systems, Chongqing University of Posts and Telecommunications, Chongqing 400065, China

* **Correspondence:** Email: zhouws@cqupt.edu.cn; Tel: +8615823257830; Fax: +8602362471796.

Abstract: This paper discussed the synchronization of impulsive fuzzy neural networks (FNNs) with uncertainty of information exchange. Since the data of neural networks (NNs) cannot be completely measured in reality, we designed an observer-based impulsive controller on the basis of the partial measurement results and achieved the purpose of reducing the communication load and the controller load of FNNs. In terms of the Lyapunov stability theory, an impulsive augmented error system (IAES) was established and two sufficient criteria to guarantee the synchronization of our FNNs system were obtained. Finally, we demonstrated the validity of the results by a numerical example.

Keywords: uncertain exchanging information; neural networks; fuzzy; impulsive; synchronization

1. Introduction

Fuzzy neural networks (FNNs) [1], which allow the activity of a neuron to be a "fuzzy" rather than an "all-or-one" process, have attracted popularity as a powerful tool for modeling complex systems due to their ability to handle uncertain and nonlienar dynamics. Recently, such neural networks (NNs) have drawn considerable attention. For example, a novel Takagi-Sugeno (T-S) fuzzy coupling NN with adjustable coupling intensity was designed [2]. In the work [3], a fuzzy pulse controller that does not need to share fuzzy parameters with FNNs has been presented. In the work [4], a topology-based fuzzy impulsive mechanism is proposed to schedule information transmission on the network for the first time, and the exponential synchronization of discrete and continuous systems are derived. Moreover, FNNs arise naturally in a number of applications, such as data compression [5], pattern recognition [6], image processing [7], adaptive signal processing [8], associative memory [9], optimization problems [10], and so on [11–14]. The advantage of FNNs is the ability to handle uncertainty and adapt to specific problems, allowing for greater flexibility than traditional NNs. Unfortunately, many existing excellent studies are about continuous-time FNNs, but there are few studies on discrete-time conditions.

The uncertainty in the information interaction NNs is unavoidable and may lead to packet dropouts, communication delay, communication error, or other problems [15–18]. In recent years, many research results have emerged around the uncertainty model of NNs. In [19], based on the event-triggered mechanism, the quasi-consensus tracking problems of uncertain multi-agent systems were studied. In [20], the synchronization conditions for NNs with bounded delay are achieved. As time goes on, robust synchronization attracted lots of attention since it became a powerful tool to study the uncertainty between coupled neural nodes [21]. In [22],

using the impulsive control and the stability theory, several criteria for local and global robust synchronization in complex dynamical networks with unknown network coupling functions are developed. In [23], global robust synchronization for the multiple memory NNs with uncertain parameters was studied by an adaptive coupling method. Therefore, it is worthful and meaningful to devise a method to make NN models with uncertain information.

In the past decades, many effective control strategies have been proposed to synchronize NNs, such as state-feedback control [24–26], adaptive control, coupling control [27], pinning control [28], and so on. Among these control methods, impulse control is one of the most practical and economical strategies since it is discontinuous. Therefore, the implementation of the controller is easier and the control cost is effective [29–31]. In recent years, many scholars have studied the synchronization of NNs based on impulse control strategies. The synchronization of nonlinear delay systems is investigated by means of event-triggered impulsive control [32], where impulsive instants are determined by a Lyapunov-based event-triggered mechanism. In [33], the Lyapunov stability of impulsive systems via event-triggered impulsive control is explored, where dynamical systems evolve depending on continuous time equations most of the time, but occasionally exhibit instantaneous jumps when impulsive events are triggered. Two sufficient criterion for the hybrid delay stochastic reaction diffusion NNs to achieve exponential synchronization are designed by an impulsive controller in [34]. Almost all the existing synchronization strategies are designed on the condition that the state of the master system is available [35]. Due to the constraints of physical systems and sensors, part states of high-order systems cannot be measured directly [36]. Therefore, it is worthy and necessary to design a new type of synchronization control strategy for FNNs by making full use of the available measurement information. In [37], asynchronous observer and fault detection algorithms are designed to tackle a hidden Markov model. Although the continuous time impulsive systems have been studied comprehensively, there are few studies on the synchronization of discrete time FNNs by using impulse control strategies; thus, it is valuable to strengthen the research in discrete-time FNNs.

Motivated by the above discussions, a discrete-time FNN (2.2) with uncertain information exchange is established, and a distributed impulsive observer-based controller (DIOBC) and impulsive augmented error system (IAES) are designed. Based on the Lyapunov method, two sufficient conditions for the model to achieve synchronization are obtained, and the validity of our results is illustrated by numerical examples. The main contributions of our article are summarized as follows:

(1) The traditional general control strategy will lead to heavy communication load and waste of controller resources due to too many control times. The impulsive controller we designed works only at the impulsive time t_m, and the FNN also interacts only at t_m time. By designing such an impulsive controller, the controller benefit is greatly improved.

(2) An impulsive controller with unknown weight information between nodes has been designed, which is the main challenge to the research of master-slave FNNs. The uncertain weights are transformed into a Laplacian matrix with bounded norm to deal with the uncertain information interaction caused by the uncertain weights of the nodes in the FNNs.

(3) The case where we only measure the state information of FNNs is considered, and through these measurements, the observer-based impulsive controller model is established. In addition, the controller with an impulsive observer also makes our synchronization analysis more complicated.

We introduce the FNNs, DIOBC and IAES in Section 2, and in Section 3, the synchronization of FNNS is proved. In Section 4, the gains about controller and observer are designed. In Section 5, a numerical example is presented to clarify the validity of the results. Our conclusion is depicted in Section 6.

Notations: $\mathbb{Z}$, $\mathbb{Z}_+$ stand for nonnegative integers and positive integers, respectively. $\mathbb{R}^n$ and $\mathbb{R}^{m\times n}$ denote the n-dimensional Euclidean space and the set of all $m\times n$ matrices. The 2-norm for a vector is expressed as $\|\cdot\|_2$. For a matrix A, its transpose, largest eigenvalue, and smallest eigenvalue are denoted by A^T, $\bar{\lambda}(A)$, and $\underline{\lambda}(A)$, respectively. The notation $*$ inside the matrix denotes the term induced by symmetry. The positive definite matrix A is represented by $A > 0$, and the notation

$A_1 - A_2 > 0$ ($A_1 - A_2 \geq 0$) means $A_1 > A_2$ ($A_1 \geq A_2$), where A_1 and A_2 are symmetric matrices. The matrix $\text{diag}_n\{\cdot\}$ stands for a diagonal matrix belonging to $\mathbb{R}^{n\times n}$. The symbol $\otimes$ stands for the Kronecker product. $a_{ij}(k) > 0, \forall i \neq j$ means that the nodes v_i and v_j can exchange information mutually. The Laplacian matrix of the connection condition is represented by $\mathcal{L}(k)$, where $\mathcal{L}_{ii}(k) = \sum_{i\neq j} a_{ij}(k)$ and $\mathcal{L}_{ij}(k) = -a_{ij}(k)$.

2. Preliminaries

2.1. FNNs description

Each node in the FNNs model needs to satisfy the following rules:

Plant Rule l: If $\xi_1(k)$ is m_{l1} and ... and $\xi_p(k)$ is m_{lp}, then

$$\begin{cases} x_i(k+1) = D_l x_i(k) + B_l g\left(x_i(k)\right) + u_i(k), \\ y_i(k+1) = C_l x_i(k), \end{cases} \tag{2.1}$$

where

$$i \in \Phi_N \triangleq \{1, 2, \ldots, N\}, \boldsymbol{x}_i(k) \in \mathbb{R}^n,$$

and $u_i(k) \in \mathbb{R}^n$ are the state and the control input of the FNNs node i, respectively. $\xi_1(k), \ldots, \xi_p(k)$ are premise variables that are functions of time, and $m_{l1}, \ldots, m_{lp}$ are the fuzzy sets for each premise variable. The index l belongs to the set

$$\Phi_l \triangleq \{1, 2, \ldots, r\},$$

where r denotes the number of fuzzy rules.

$$g\left(x_i(k)\right) = \left[g_1\left(x_{i1}(k)\right), g_2\left(x_{i2}(k)\right), \ldots, g_n\left(x_{in}(k)\right)\right]^T$$

represents the nonlinear activation functions, and the matrix

$$D_l = \text{diag}_n\{d_{l1}, \ldots, d_{ln}\} \in \mathbb{R}^{n\times n}, \quad B_l \in \mathbb{R}^{n\times n}, \quad C_l \in \mathbb{R}^{n\times m}$$

of FNNs is the matrix of coefficients, that we know.

Integrate all the nodes together, and the FNNs (2.1) can be given as

$$\begin{cases} x_i(k+1) = \sum_{l=1}^{r} \theta_l(k)\left\{D_l x_i(k) + B_l g\left(x_i(k)\right)\right\} + u_i(k), \\ y_i(k+1) = \sum_{l=1}^{r} \theta_l(k) C_l x_i(k), \end{cases} \tag{2.2}$$

where $\theta_l(k)$ satisfies

$$\theta_l(k) = \frac{\prod_{\iota=1}^{p} m_{l\iota}\left(\xi_\iota(k)\right)}{\sum_{j=1}^{r}\prod_{\iota=1}^{p} m_{j\iota}\left(\xi_\iota(k)\right)}$$

with

$$\sum_{l=1}^{r} \theta_l(k) = 1,$$

and $m_{l\iota}\left(\xi_\iota(k)\right)$ is the grade of membership of $\xi_\iota(k)$ in

$$m_{l\iota}, \iota \in \Phi_p \triangleq \{1, 2, \ldots, p\}.$$

Define $s(k)$ as the trajectory, which the FNNs (2.2) aim to follow:

$$\begin{cases} s(k+1) = \sum_{l=1}^{r} \theta_l(k)\left\{D_l s(k) + B_l g\left(s(k)\right)\right\}, \\ y_s(k+1) = \sum_{l=1}^{r} \theta_l(k) C_l s(k), \end{cases} \tag{2.3}$$

where $g\left(s(k)\right)$ is an activation function and satisfies the following assumption.

Assumption 2.1. *The functions*

$$g_j(\cdot), j \in \Phi_n \triangleq \{1, 2, \ldots, n\}$$

satisfy $g_j(0) = 0$, *and there exist the constants* $\bar{\vartheta}_j$ *and* $\underline{\vartheta}_j$ *such that*

$$\underline{\vartheta}_j \leq \frac{g_j(\chi_1) - g_j(\chi_2)}{\chi_1 - \chi_2} \leq \bar{\vartheta}_j, \tag{2.4}$$

where the constants $\chi_1, \chi_2 \in \mathbb{R}$ *satisfy* $\chi_1 \neq \chi_2$.

Remark 2.1. *Each state $s(k)$ is a target signal of FNNs (2.2) to achieve synchronization by using the leader-follower method [38]. In [39], the T-S fuzzy logic is used to study the synchronization of master-slave NNs in terms of fuzzy rules to tackle local linear representation of nonlinear systems. Founded on the above, we investigate the synchronization of a group of master-slave NNs with n nodes. It is worth noting that most of the existing works assume that the states of FNNs (2.2) and unforced FNNs (2.3) are available, whereas in reality, due to the constraints of physical systems and sensors, only partial states of the FNNs (2.2) and (2.3) can be measured.*

2.2. DIOBC

The continuous-time control causes problems such as high communication loads and low controller efficiency. In this section, an observer-based impulsive controller is designed to optimize these problems. The impulsive instants are denoted as

$$\{t_m\}, \quad m \in \mathbb{Z}. \tag{2.5}$$

Define $t_0 = -1$. The impulsive intervals $\tau_m, m \in \mathbb{Z}_+$ satisfy

$$\tau_m \triangleq t_m - t_{m-1}.$$

Before arguing our main conclusions, we need the following assumption:

Assumption 2.2. *The interval $\tau_m, m \in \mathbb{Z}_+$ satisfies*

$$0 < \tau_m \leq \tau. \tag{2.6}$$

Based on the partial information obtained from FNNs measurements, the following observers were designed. For the non-impulsive instants k, the observers are given as follows:

$$\begin{cases} \hat{x}_i(k+1) = \sum_{l=1}^{r} \theta_l(k) \{D_l \hat{x}_i(k) + B_l g(\hat{x}_i(k))\}, \\ \hat{s}(k+1) = \sum_{l=1}^{r} \theta_l(k) \{D_l \hat{s}(k) + A_l g(\hat{s}(k))\}, \end{cases} \tag{2.7}$$

where $\hat{x}_i(k)$ and $\hat{s}(k)$ are observer states of FNNs (2.2) and (2.3), respectively.

Furthermore, at the impulsive instants t_m, the observer model is

$$\begin{cases} \hat{s}(t_m+1) = \hat{s}(t_m) + \sum_{n=1}^{r} \theta_n(t_m) \{R_{sn}(y_s(t_m) - \hat{y}_s(t_m))\}, \\ \hat{x}_i(t_m+1) = \hat{x}_i(t_m) + \sum_{n=1}^{r} \theta_n(t_m) \{R_{in}(y_i(t_m) - \hat{y}_i(t_m))\} \\ \qquad\qquad + u_i(t_m), \end{cases} \tag{2.8}$$

where $R_{sn} \in \mathbb{R}^{n\times m}$ and $R_{in} \in \mathbb{R}^{n\times m}$ are observer gains.

Remark 2.2. *Using available measurement values to estimate the system state is an important technique in the field of control. In [40], Cheng et al. designed an asynchronous state observer by using a hidden Markov model and obtained sufficient conditions for the existence of a fuzzy asynchronous fault detection filter for a class of nonlinear Markov jump systems. However, the system state may not be fully accessible. In this case, we need to construct an observer and establish a corresponding tracking error system between the observer and the target. It should be noted that the system (2.2) under the control input $u_i(t)$ is a type of pulse system. Therefore, in order to build a suitable tracking error system, it is natural to consider the observer with impulse effect.*

Based on the observer model given above, we design the following impulsive controller. With $u(k) = 0$ at the non-impulsive instants k and at the instants t_m, our FNNs of the node i are given as

$$\begin{aligned} u_i(t_m) = \sum_{l=1}^{r} \theta_l(t_m) \Big\{ & K_{il} \sum_{j=1}^{N} a_{ij}(t_m) \hat{x}_j(t_m) \\ & + \varsigma_i H_{il} (\hat{x}_i(t_m) - \hat{s}(t_m)) \\ & + M_{il} \sum_{j=1}^{N} a_{ij}(t_m) y_j(t_m) \\ & + \varsigma_i F_{il} (y_i(t_m) - y_s(t_m)) \Big\}, \end{aligned} \tag{2.9}$$

where matrices $K_{il} \in \mathbb{R}^{n\times n}, H_{il} \in \mathbb{R}^{n\times n}, M_{il} \in \mathbb{R}^{n\times m}$, $F_{il} \in \mathbb{R}^{n\times m}$, and $\varsigma_i \geq 0$ are the controller gain and pinning gain respectively.

Remark 2.3. *As far as we know, most of the synchronization controllers used in NNs depend on the state information of the master-slave systems. However, the synchronization of FNNs are derived based on the the coupling effect between nodes and an uncertain information impulsive controller [41]. Motivated by this method, we employ the fuzzy theory to describe the nonlinear model and design a fuzzy uncertain information impulsive controller.*

2.3. IAES and preliminaries

The uncertainty of the connection weight $a_{ij}(k)$, $i, j \in \Phi_N$ between the nodes of FNNs will lead to uncertain information interaction. In order to deal with this problem, we assume that these connection weights will vary over an interval, that is,

$$0 \leq \underline{a}_{ij} \leq a_{ij}(k) \leq \bar{a}_{ij}, \quad i \neq j. \tag{2.10}$$

To solve the problem of uncertain node weights, we introduce the following notations:

$$\begin{aligned}\check{a}_{ij} &= \begin{cases} \frac{1}{2}\sum_{j=1,i\neq j}^{N}\left(\underline{a}_{ij}+\bar{a}_{ij}\right), & i=j,\\ -\frac{1}{2}\left(\underline{a}_{ij}+\bar{a}_{ij}\right), & i\neq j,\end{cases}\\ \hat{a}_{ij} &= \begin{cases} \frac{1}{2}\sum_{j=1,i\neq j}^{N}\left(\underline{a}_{ij}-\bar{a}_{ij}\right), & i=j,\\ -\frac{1}{2}\left(\underline{a}_{ij}-\bar{a}_{ij}\right), & i\neq j.\end{cases}\end{aligned} \tag{2.11}$$

Through the above discussion, the uncertain connection weight (2.10) can be rewritten as

$$a_{ij}(k) = \check{a}_{ij} + \hat{a}_{ij}\Lambda_l(k), \tag{2.12}$$

where the index is

$$l = N(i-1)+j,$$

and the time-varying scalar $\Lambda_l(k)$ satisfies

$$-I \leq \Lambda_l(k) \leq I.$$

The Laplacian matrix of the distributed protocol is expressed as

$$\mathcal{L}(k) = \mathcal{L} + \Delta\mathcal{L}(k) = \mathcal{L} + M\Lambda(k)N, \tag{2.13}$$

where

$$\begin{aligned}\mathcal{L} &= \begin{bmatrix} \check{a}_{11} & \check{a}_{12} & \dots & \check{a}_{1N}\\ \check{a}_{21} & \check{a}_{22} & \dots & \check{a}_{2N}\\ \vdots & \vdots & \ddots & \vdots\\ \check{a}_{N1} & \check{a}_{N2} & \dots & \check{a}_{NN}\end{bmatrix},\\ M &= \left[\sqrt{\hat{a}_{11}}e_1, \sqrt{\hat{a}_{12}}e_1, \dots, \sqrt{\hat{a}_{1N}}e_1, \dots, \sqrt{\hat{a}_{N1}}e_N, \dots, \sqrt{\hat{a}_{NN}}e_N\right] \in \mathbb{R}^{N\times N^2},\\ N &= \left[\sqrt{\hat{a}_{11}}e_1, \sqrt{\hat{a}_{12}}e_2, \dots, \sqrt{\hat{a}_{1N}}e_N, \dots, \sqrt{\hat{a}_{N1}}e_1, \dots, \sqrt{\hat{a}_{NN}}e_N\right]^T \in \mathbb{R}^{N^2\times N},\\ e_i &= [\underbrace{0,\dots,0}_{i-1},1,\underbrace{0,\dots,0}_{N-i}]^T,\\ \Lambda(k) &= \mathrm{diag}_{N^2}\left\{\Lambda_1(k),\Lambda_2(k),\dots,\Lambda_{N^2}(k)\right\}.\end{aligned}$$

We denote the estimation error of the leader FNNs, the state error, and the estimation error between the leader FNNs (2.3) and the FNNs node i as

$$\boldsymbol{e}_s(k) \triangleq s(k) - \hat{s}(k), \quad \boldsymbol{e}_i(k) \triangleq \boldsymbol{x}_i(k) - s(k)$$

and

$$\hat{\boldsymbol{e}}_i(k) \triangleq \hat{\boldsymbol{x}}_i(k) - \hat{s}(k),$$

respectively. Furthermore, the augmented state

$$\eta_i(k) = \left[\boldsymbol{e}_s^T(k)\ \boldsymbol{e}_i^T(k)\ \hat{\boldsymbol{e}}_i^T(k)\right]^T$$

is defined. By integrating the formulae (2.2), (2.3), (2.8), (2.9), and (2.12), we have

$$\eta_i(k+1) = \begin{cases} \sum_{l=1}^{r}\theta_l(k)\left\{(I_3\otimes D_l)\,\eta_i(k)\right.\\ \left.+(I_3\otimes B_l)\,\overline{g}\left(\eta_i(k)\right)\right\}, & k\neq t_m,\\ \sum_{l=1}^{r}\theta_l(t_m)\sum_{n=1}^{r}\theta_n(t_m)\\ \times\left\{\bar{D}\eta_i(t_m)+(I_3\otimes B_{ln})\,\overline{g}\left(\eta_i(t_m)\right)\right.\\ \left.+\bar{K}\sum_{j=1}^{N}\mathcal{L}_{ij}\eta_j(t_m)\right\}, & k=t_m,\end{cases} \tag{2.14}$$

where

$$\begin{aligned}\bar{K} &= \begin{bmatrix} 0 & 0 & 0\\ 0 & M_{in}C_l & K_{in}\\ 0 & M_{in}C_l & K_{in}\end{bmatrix},\\ \overline{g}\left(\eta_i(k)\right) &= \begin{bmatrix} g\left(s(k)\right)-g\left(\hat{s}(k)\right)\\ g\left(\boldsymbol{x}_i(k)\right)-g\left(s(k)\right)\\ g\left(\hat{\boldsymbol{x}}_i(k)\right)-g\left(\hat{s}(k)\right)\end{bmatrix},\\ D_{11} &= \begin{bmatrix} D_l - R_{sn}C_l & 0\\ 0 & D_l+\varsigma_i F_{in}C_l\end{bmatrix},\\ D_{12} &= \begin{bmatrix} 0 & \varsigma_i H_{in}\end{bmatrix}^T,\\ D_{21} &= \begin{bmatrix} R_{in}C_l - R_{sn}C_l & R_{in}C_l+\varsigma_i F_{in}C_l\end{bmatrix},\\ D_{22} &= D_l - R_{in}C_l + \varsigma_i H_{in},\\ \bar{D} &= \begin{bmatrix} D_{11} & D_{12}\\ D_{21} & D_{22}\end{bmatrix}.\end{aligned}$$

Considering the system (2.14) and defining the augmented error state

$$\eta(k) = \left[\ \boldsymbol{e}_s^T(k)\ \boldsymbol{e}_1^T(k)\ \hat{\boldsymbol{e}}_1^T(k)\ \dots\ \boldsymbol{e}_N^T(k)\ \hat{\boldsymbol{e}}_N^T(k)\ \right]^T,$$

we have the following IAES:

$$\eta(k+1) = \begin{cases} \sum_{l=1}^{r}\theta_l(k)\left\{(I_{2N+1}\otimes D_l)\,\eta(k)\right.\\ \left.+(I_{2N+1}\otimes B_l)\,g(\eta(k))\right\}, & k\neq t_m,\\ \sum_{l=1}^{r}\theta_l(k)\sum_{n=1}^{r}\theta_n(k)\left\{\mathcal{D}_{ln}\eta(k)\right.\\ \left.+(I_{2N+1}\otimes B_l)\,g(\eta(k))\right\}, & k=t_m,\end{cases} \tag{2.15}$$

where

$$\begin{aligned}
\mathcal{D}_{ln} &= (\mathcal{D}_1 + \mathcal{M}((\mathcal{L}+\Delta\mathcal{L})\otimes I_{2m})C \\
&\quad +\mathcal{K}((\mathcal{L}+\Delta\mathcal{L})\otimes I_{2n})\mathcal{I}), \\
\mathcal{D}_1 &= \begin{bmatrix} D_l - R_{sn}C_l & 0 \\ \mathcal{R} & \mathcal{D}_{22} \end{bmatrix}, \\
\bar{R}_i &= \begin{bmatrix} 0 \\ R_{in}C_l - R_{sn}C_l \end{bmatrix}, \\
\mathcal{D}_{22} &= \mathrm{diag}_N\{\mathcal{D}_{221}, \mathcal{D}_{222}, \ldots, \mathcal{D}_{22N}\}, \\
\mathcal{D}_{22i} &= \begin{bmatrix} D_l + \varsigma_i F_{in}C_l & \varsigma_i H_{in} \\ R_{in}C_l + \varsigma_i F_{in}C_l & D_l - R_{in}C_l + \varsigma_i H_{in} \end{bmatrix}, \\
\mathcal{R} &= \begin{bmatrix} \bar{R}_{1n}^T & \bar{R}_{2n}^T & \ldots & \bar{R}_{Nn}^T \end{bmatrix}^T, \\
\mathcal{K} &= \begin{bmatrix} 0 & \mathcal{K}_{12}^T \end{bmatrix}^T, \\
\mathcal{K}_{12} &= \mathrm{diag}_N\{\mathcal{K}_{121}, \mathcal{K}_{122}, \ldots, \mathcal{K}_{12N}\}, \\
\mathcal{M} &= \begin{bmatrix} 0 & \mathcal{M}_{12}^T \end{bmatrix}^T, \quad \mathcal{I} = \begin{bmatrix} 0 & I_N \otimes \bar{I} \end{bmatrix}, \\
\mathcal{M}_{12} &= \mathrm{diag}_N\{\mathcal{M}_{121}, \mathcal{M}_{122}, \ldots, \mathcal{M}_{12N}\}, \\
\mathcal{K}_{12i} &= \begin{bmatrix} 0 & K_{in} \\ 0 & K_{in} \end{bmatrix}, \quad \bar{I} = \begin{bmatrix} 0 & 0 \\ 0 & I_n \end{bmatrix}, \\
\mathcal{M}_{12i} &= \begin{bmatrix} M_{in} & 0 \\ M_{in} & 0 \end{bmatrix}, \ C = \begin{bmatrix} 0 & C_{12} \end{bmatrix}, \\
C_{12} &= \mathrm{diag}_N\{C_{121}, C_{122}, \ldots, C_{12N}\}, \\
C_{12i} &= \mathrm{diag}_2\{C_l, 0\}, \quad \tilde{g}(e_s(k)) = g(s(k)) - g(\hat{s}(k)), \\
g(\eta(k)) &= \left[\tilde{g}^T(e_s(k))\ \tilde{g}^T(\eta_1(k))\ \ldots\ \tilde{g}^T(\eta_N(k))\right]^T, \\
\tilde{g}(\eta_i(k)) &= \begin{bmatrix} g(\boldsymbol{x}_i(k)) - g(s(k)) \\ g(\hat{\boldsymbol{x}}_i(k)) - g(\hat{s}(k)) \end{bmatrix}.
\end{aligned}$$

Remark 2.4. *Since the information exchange between the large-scale biological system and the artificial system is not fixed, the robustness of the coupling system connection weight is very important. In order to describe the uncertainty of connection weights between FNN nodes in more detail, the interval uncertainty model (2.12) is introduced here.*

For the third part of the proof, we give the following definition and lemma.

Definition 2.1. *[42] The synchronization of FNNs (2.2) and (2.3) will be arrived if the following inequality holds*

$$\lim_{k\to\infty} \|\eta(k)\|_2 = 0. \tag{2.16}$$

Lemma 2.1. *[43] For a real matrix $\Xi = \Xi^T$, the following assertions are equivalent*

$$\begin{aligned}
&\Xi := \begin{pmatrix} \Xi_{11} & \Xi_{12} \\ * & \Xi_{22} \end{pmatrix} < 0, \\
&\Xi_{11} < 0, \Xi_{22} - \Xi_{12}^T \Xi_{11}^{-1} \Xi_{12} < 0, \\
&\Xi_{22} < 0, \Xi_{11} - \Xi_{12} \Xi_{22}^{-1} \Xi_{12}^T < 0.
\end{aligned}$$

3. Main results

In this section, sufficient conditions for the synchronization of FNNs (2.2) with the trajectory (2.3) are presented.

Theorem 3.1. *Suppose that the scalars α_1 and α_2 satisfy $0 < \alpha_2 < 1 \le \alpha_1$. FNNs (2.2) are said to be synchronized with (2.3) if there exist matrices $P_l > 0, \hat{\epsilon}_1 > 0$, $F_{in}, H_{in}, K_{in}, M_{in}, R_{sn}$, and R_{in} and Conditions (3.1)–(3.3) hold for $\forall\sigma \in \Phi_l$:*

$$\begin{bmatrix} -\alpha_1 P_l - \overline{\mathcal{T}}_1\hat{\epsilon}_1 & \overline{\mathcal{T}}_2\hat{\epsilon}_1 & (I_{2N+1}\otimes D_l)^T P_l \\ * & -\hat{\epsilon}_1 & (I_{2N+1}\otimes B_l)^T P_l \\ * & * & -P_\sigma \end{bmatrix} < 0, \tag{3.1}$$

$$\begin{bmatrix} -\alpha_2 P_l - \overline{\mathcal{I}}_1\hat{\epsilon}_1 & \overline{\mathcal{T}}_2\hat{\epsilon}_1 & \mathcal{D}^T \\ * & -\hat{\epsilon}_1 & (I_{2N+1}\otimes B_l)^T \\ * & * & -P_\sigma^{-1} \end{bmatrix} < 0, \tag{3.2}$$

$$(\tau - 1)\ln\alpha_1 + \ln\alpha_2 < 0, \tag{3.3}$$

where

$$\begin{aligned}
\overline{\mathcal{T}}_1 &= \mathrm{diag}_{2N+1}\{T_1, T_1, \ldots, T_1\}, \\
\overline{\mathcal{T}}_2 &= \mathrm{diag}_{2N+1}\{T_2, T_2, \ldots, T_2\}, \\
T_1 &= \mathrm{diag}_n\left\{\underline{\vartheta}_1\bar{\vartheta}_1, \underline{\vartheta}_2\bar{\vartheta}_2, \ldots, \underline{\vartheta}_n\bar{\vartheta}_n\right\}, \\
T_2 &= \mathrm{diag}_n\left\{\frac{\vartheta_1+\bar{\vartheta}_1}{2}, \frac{\underline{\vartheta}_2+\bar{\vartheta}_2}{2}, \ldots, \frac{\underline{\vartheta}_n+\bar{\vartheta}_n}{2}\right\}, \\
\hat{\epsilon}_1 &= \mathrm{diag}_{2N+1}\{\epsilon_1, \epsilon_1, \ldots, \epsilon_1\}, \\
\epsilon_1 &= \mathrm{diag}_n\{\epsilon_{11}, \epsilon_{12}, \ldots, \epsilon_{1n}\}.
\end{aligned}$$

Proof. Based on DIOBC and IAES, we establish the following Lyapunov functional

$$\mathcal{V}(\eta(k), k) = \eta^T(k)(\sum_{l=1}^{r} \theta_\sigma(k) P_\sigma)\eta(k), \tag{3.4}$$

where $P_\sigma > 0$, $\forall\sigma \in \Phi_l$, and for the sake of simplicity, we use $\mathcal{V}(k)$ to represent $\mathcal{V}(\eta(k), k)$. □

Next, we demonstrate the synchronization of FNNs (2.2) with the next three steps.

Step 1. When $k \neq t_m$, we define the Lyapunov functional (3.4) as

$$\Delta\mathcal{V}(k) \triangleq \mathcal{V}(k+1) - \alpha_1\mathcal{V}(k). \tag{3.5}$$

By substituting the IAES (2.15) into (3.5), we obtain

$$\begin{aligned}
&\Delta\mathcal{V}(k)\\
&=\sum_{\sigma=1}^{r}\theta_\sigma(k+1)\sum_{l=1}^{r}\theta_l(k)\\
&\quad\times\left\{\eta^T(k+1)^TP_\sigma\eta(k+1)-\alpha_1\eta^T(k)P_l\eta(k)\right\}\\
&=\sum_{\sigma=1}^{r}\theta_\sigma(k+1)\sum_{l=1}^{r}\theta_l(k)\sum_{n=1}^{r}\theta_j(k)\\
&\quad\times\left\{\left(\eta^T(k)\left(I_{2N+1}\otimes D_l\right)^T+g^T(\eta(k))\left(I_{2N+1}\otimes B_l\right)^T\right)\right.\\
&\quad\times P_\sigma\left(\left(I_{2N+1}\otimes D_n\right)\eta(k)+\left(I_{2N+1}\otimes B_n\right)g(\eta(k))\right)\\
&\quad\left.-\alpha_1\eta^T(k)P_l\eta(k)\right\}\\
&\le\sum_{\sigma=1}^{r}\theta_\sigma(k+1)\sum_{l=1}^{r}\theta_l(k)\\
&\quad\times\left\{\left(\eta^T(k)\left(I_{2N+1}\otimes D_l\right)^T+g^T(\eta(k))\left(I_{2N+1}\otimes B_l\right)^T\right)\right.\\
&\quad\times P_\sigma\left(\left(I_{2N+1}\otimes D_l\right)\eta(k)+\left(I_{2N+1}\otimes B_l\right)g(\eta(k))\right)\\
&\quad\left.-\alpha_1\eta^T(k)P_l\eta(k)\right\}\\
&=\sum_{\sigma=1}^{r}\theta_\sigma(k+1)\sum_{l=1}^{r}\theta_l(k)\\
&\quad\times\left\{\eta^T(k)\left(I_{2N+1}\otimes D_l\right)^TP_\sigma\left(I_{2N+1}\otimes D_l\right)\eta(k)\right.\\
&\quad+\eta^T(k)\left(I_{2N+1}\otimes D_l\right)^TP_\sigma\left(I_{2N+1}\otimes B_l\right)g(\eta(k))\\
&\quad+\eta(k)\left(I_{2N+1}\otimes D_l\right)P_\sigma g^T(\eta(k))\left(I_{2N+1}\otimes B_l\right)^T\\
&\quad+g^T(\eta(k))\left(I_{2N+1}\otimes B_l\right)^TP_\sigma\left(I_{2N+1}\otimes B_l\right)g(\eta(k))\\
&\quad\left.-\alpha_1\eta^T(k)P_l\eta(k)\right\}\\
&=\sum_{\sigma=1}^{r}\theta_\sigma(k+1)\sum_{l=1}^{r}\theta_l(k)\left\{\zeta^T(k)\Omega_{\sigma l}\zeta(k)\right\},
\end{aligned} \tag{3.6}$$

where

$$\begin{aligned}
\Omega_{\sigma l}&=\begin{bmatrix}\Omega_{111}-\alpha_1P_\sigma & \Omega_{112}\\ * & \Omega_{122}\end{bmatrix},\\
\Omega_{111}&=\left(I_{2N+1}\otimes D_l\right)^TP_\sigma\left(I_{2N+1}\otimes D_l\right),\\
\Omega_{112}&=\left(I_{2N+1}\otimes D_l\right)^TP_\sigma\left(I_{2N+1}\otimes B_l\right),\\
\Omega_{122}&=\left(I_{2N+1}\otimes B_l\right)^TP_\sigma\left(I_{2N+1}\otimes B_l\right),\\
\zeta(k)&=\begin{bmatrix}\eta^T(k) & g^T(\eta(k))\end{bmatrix}^T.
\end{aligned}$$

Combining with Assumption 2.1, we obtain the inequalities (3.7) and (3.8) about the functions $g_j(\cdot)$, $j\in\Phi_N$ for any scalar $\epsilon_{1j}>0$

$$\epsilon_{1j}\left(g_j\left(\boldsymbol{x}_{ij}(k)\right)-\underline{\vartheta}_j\boldsymbol{x}_{ij}(k)\right)\left(g_j\left(\boldsymbol{x}_{ij}(k)\right)-\bar{\vartheta}_j\boldsymbol{x}_{ij}(k)\right)\le 0, \tag{3.7}$$

$$\epsilon_{1j}\left(g_j\left(\hat{\boldsymbol{x}}_{ij}(k)\right)-\underline{\vartheta}_j\hat{x}_{ij}(k)\right)\left(g_j\left(\hat{\boldsymbol{x}}_{ij}(k)\right)-\bar{\vartheta}_j\hat{\boldsymbol{x}}_{ij}(k)\right)\le 0. \tag{3.8}$$

By combining with inequalities (3.7) and (3.8), we get that the following (3.9) holds for any $\epsilon_1>0$

$$\hat{\epsilon}_1(g(\eta(k))-\underline{\check{\vartheta}}\eta(k))^T(g(\eta(k))-\hat{\bar{\vartheta}}\eta(k))\le 0, \tag{3.9}$$

where

$$\begin{aligned}
\underline{\check{\vartheta}}&=\mathrm{diag}_{2N+1}\{\underline{\hat{\vartheta}},\underline{\hat{\vartheta}},\ldots,\underline{\hat{\vartheta}}\},\\
\underline{\hat{\vartheta}}&=\mathrm{diag}_n\left\{\underline{\vartheta}_1,\underline{\vartheta}_2,\ldots,\underline{\vartheta}_n\right\},\\
\hat{\bar{\vartheta}}&=\mathrm{diag}_{2N+1}\{\hat{\bar{\vartheta}},\hat{\bar{\vartheta}},\ldots,\hat{\bar{\vartheta}}\},\\
\hat{\bar{\vartheta}}&=\mathrm{diag}_n\left\{\bar{\vartheta}_1,\bar{\vartheta}_2,\ldots,\bar{\vartheta}_n\right\}.
\end{aligned}$$

According to the inequality of the activation function (3.9), it follows that

$$\zeta^T(k)\begin{bmatrix}\overline{\mathcal{T}}_1\hat{\epsilon}_1 & -\overline{\mathcal{T}}_2\hat{\epsilon}_1\\ * & \hat{\epsilon}_1\end{bmatrix}\zeta(k)\le 0. \tag{3.10}$$

The difference is that (3.5) satisfies the following inequality (3.11) by taking (3.6) into (3.10):

$$\Delta\mathcal{V}(k)\le\sum_{\sigma=1}^{r}\theta_\sigma(k+1)\sum_{l=1}^{r}\theta_l(k)\left\{\zeta^T(k)\Omega_{\sigma l2}\zeta(k)\right\}, \tag{3.11}$$

where

$$\Omega_{\sigma l2}=\begin{bmatrix}\Omega_{111}-\alpha_1P_l-\overline{\mathcal{T}}_1\hat{\epsilon}_1 & \Omega_{112}+\overline{\mathcal{T}}_2\hat{\epsilon}_1\\ * & \Omega_{122}-\hat{\epsilon}_1\end{bmatrix}.$$

Pre-multiplying and post-multiplying the inequality condition (3.1) with $\mathrm{diag}_3\{I,I,P\}$ and applying Lemma 2.1, we have $\Omega_{\sigma l2}<0$, that is,

$$\mathcal{V}(k+1)<\alpha_1\mathcal{V}(k). \tag{3.12}$$

Step 2. When the time is $k=t_m$, we define the Lyapunov functional (3.4) as:

$$\Delta\mathcal{V}(t_m)=\mathcal{V}(t_m+1)-\alpha_2\mathcal{V}(t_m). \tag{3.13}$$

Putting the IAES (2.15) into (3.13), we obtain

$$\begin{aligned}
&\Delta\mathcal{V}(t_m)\\
&=\sum_{\sigma=1}^{r}\theta_\sigma(t_m+1)\sum_{l=1}^{r}\theta_l(t_m)\\
&\quad\times\left\{\eta^T(t_m+1)P_\sigma\eta(t_m+1)-\alpha_2\eta^T(t_m)P_l\eta(t_m)\right\}\\
&=\sum_{\sigma=1}^{r}\theta_\sigma(t_m+1)\sum_{l=1}^{r}\theta_l(t_m)\sum_{n=1}^{r}\theta_n(t_m)\sum_{a=1}^{r}\theta_a(t_m)\\
&\quad\sum_{b=1}^{r}\theta_b(t_m)\cdot\left\{g^T(\eta(t_m))\left(\mathcal{D}_{ln}\eta(t_m)+(I_{2N+1}\otimes B_l)\right)^T\right.\\
&\quad\times p_\sigma\left(\mathcal{D}_{ab}\eta(t_m)+(I_{2N+1}\otimes B_a)\,g(\eta(t_m))\right)\\
&\quad\left.-\alpha_2\eta^T(t_m)P_l\eta(t_m)\right\}\\
&\le\sum_{\sigma=1}^{r}\theta_\sigma(t_m+1)\sum_{l=1}^{r}\theta_l(t_m)\sum_{n=1}^{r}\theta_n(t_m)\\
&\quad\times\left\{g^T(\eta(t_m))\left(\mathcal{D}_{ln}\eta(t_m)+(I_{2N+1}\otimes B_l)\right)^T\right.\\
&\quad\times p_\sigma\left(\mathcal{D}_{ln}\eta(t_m)+(I_{2N+1}\otimes B_l)\,g(\eta(t_m))\right)\\
&\quad\left.-\alpha_2\eta^T(t_m)P_l\eta(t_m)\right\}\\
&=\sum_{\sigma=1}^{r}\theta_\sigma(t_m+1)\sum_{l=1}^{r}\theta_l(t_m)\sum_{n=1}^{r}\theta_n(t_m)\cdot\left\{\eta^T(t_m)\right.\\
&\quad\cdot\mathcal{D}_{ln}^TP_\sigma\mathcal{D}_{ln}\eta(t_m)+2\eta^T(t_m)\mathcal{D}_{ln}P_\sigma\left(I_{2N+1}\otimes B_l\right)\\
&\quad\cdot g(\eta(t_m))+g^T(\eta(t_m))\left(I_{2N+1}\otimes B_l\right)^TP_\sigma\left(I_{2N+1}\otimes B_l\right)\\
&\quad\left.\cdot g(\eta(t_m))-\alpha_2\eta^T(t_m)P_l\eta(t_m)\right\}.
\end{aligned}\tag{3.14}$$

Combining inequalities of the activation function (3.10) and the difference functional (3.14), we have

$$\begin{aligned}
\Delta\mathcal{V}(k)\le&\sum_{\sigma=1}^{r}\theta_\sigma(t_m+1)\sum_{l=1}^{r}\theta_l(t_m)\sum_{n=1}^{r}\theta_n(t_m)\\
&\times\left\{\zeta^T(k)\Omega_{\sigma ln}\zeta(k)\right\},
\end{aligned}\tag{3.15}$$

where

$$\begin{aligned}
\Omega_{\sigma ln}&=\begin{bmatrix}\Omega_{311}&\Omega_{312}\\ *&\left(I_{2N+1}\otimes B_l\right)^TP_l\left(I_{2N+1}\otimes B_l\right)-\hat{\epsilon}_1\end{bmatrix},\\
\Omega_{311}&=\mathcal{D}_{ln}^TP_l\mathcal{D}_{ln}-\alpha_2P_\sigma-\overline{\mathcal{T}}_1\hat{\epsilon}_1,\\
\Omega_{312}&=\mathcal{D}_{ln}^TP_l\left(I_{2N+1}\otimes B_l\right)+\overline{\mathcal{T}}_2\hat{\epsilon}_1.
\end{aligned}$$

Applying Lemma 2.1 to (3.2), the inequality (3.16) holds with (3.15)

$$\mathcal{V}(t_m+1)<\alpha_2\mathcal{V}(t_m).\tag{3.16}$$

Step 3. Based on the above two steps, we discuss the synchronization for the FNNs (2.2).

We obtain that the following inequalities hold for $k\in(0,t_1]$ by the inequality (3.12) and Assumption 2.2

$$\mathcal{V}(k)<\alpha_1\mathcal{V}(k-1)<\cdots<\alpha_1^k\mathcal{V}(0)\le\alpha_1^{\tau-1}\mathcal{V}(0).\tag{3.17}$$

According to the inequalities (3.16) and (3.17), the inequality (3.18) is derived at the instant $k=t_1+1$.

$$\mathcal{V}(t_1+1)<\alpha_2\alpha_1^{\tau-1}\mathcal{V}(0).\tag{3.18}$$

For instants $k\in(t_1+1,t_2]$, it follows from (3.12) and (3.17) that

$$\begin{aligned}
\mathcal{V}(k)&<\alpha_1\mathcal{V}(k-1)\\
&<\cdots<\alpha_1^{k-(t_1+1)}\mathcal{V}(t_1+1)\\
&<\alpha_1^{\tau-1}\mathcal{V}(t_1+1)\\
&<\alpha_2\alpha_1^{2\tau-2}\mathcal{V}(0).
\end{aligned}\tag{3.19}$$

In view of (3.16) and (3.19), we have the following inequality at instant $k=t_2+1$

$$\mathcal{V}(t_2+1)<\alpha_2^2\alpha_1^{2\tau-2}\mathcal{V}(0).\tag{3.20}$$

By combining the formulas (3.17) to (3.20), the inequality (3.21) will hold for $\forall m\in\mathbb{Z}$

$$\mathcal{V}(t_m+1)<\left(\alpha_2\alpha_1^{\tau-1}\right)^m\mathcal{V}(0),\tag{3.21}$$

and the inequality (3.21) implies that

$$\underline{\lambda}(P)\left\|\eta\left(t_m+1\right)\right\|_2^2<\left(\alpha_2\alpha_1^{\tau-1}\right)^m\bar{\lambda}(P)\|\eta(0)\|_2^2.$$

Furthermore, we have

$$\left\|\eta\left(t_m+1\right)\right\|_2^2<\frac{\bar{\lambda}(P)}{\underline{\lambda}(P)}\left(\alpha_2\alpha_1^{\tau-1}\right)^m\|\eta(0)\|_2^2.\tag{3.22}$$

Due to $1\le\alpha_1$ and $0<\alpha_2<1$, it follows that

$$0<\alpha_2\alpha_1^{\tau-1}.\tag{3.23}$$

By the inequality (3.3), one can derive that

$$\alpha_2\alpha_1^{\tau-1}=e^{\ln\alpha_2\alpha_1^{\tau-1}}=e^{(\tau-1)\ln\alpha_1+\ln\alpha_2}<1.\tag{3.24}$$

On the basis of Definition 2.1 and inequalities (3.22)–(3.24), we get that the state is exponentially stable at instants $t_m+1, m\in\mathbb{Z}_+$, which implies

$$\lim_{m\to\infty}\left\|\eta\left(t_m+1\right)\right\|_2=0.\tag{3.25}$$

Through comparing with the inequalities (3.17) and (3.19) and combining with the inequality (3.22), we can derive the following inequality $\forall k \in (t_m + 1, t_{m+1}], m \in \mathbb{Z}$

$$\|\eta(k)\|_2 < \sqrt{\frac{\bar{\lambda}(P)}{\underline{\lambda}(P)}\alpha_1^{\tau-1}}\,\|\eta(t_m+1)\|_2\,. \tag{3.26}$$

Due to the term $(\bar{\lambda}(P)/\underline{\lambda}(P))\alpha_1^{\tau-1}$ being bounded, the following conditions exist $\forall k \in (t_m + 1, t_{m+1}], m \in \mathbb{Z}$

$$\lim_{k\to\infty}\|\eta(k)\|_2 < \sqrt{\frac{\bar{\lambda}(P)}{\underline{\lambda}(P)}\alpha_1^{\tau-1}}\,\lim_{m\to\infty}\|\eta(t_m+1)\|_2 = 0.$$

Taking account of (3.25) and (3.26), we have

$$\lim_{k\to\infty}\|\eta(k)\| = 0,$$

which implies that the synchronization of FNNs (2.2) are achieved.

4. Observer and controller gains design

In this section, we design the gains of an impulsive observer and controller on the conclusions of Part III.

Theorem 4.1. *Given scalars $0 < \alpha_2 < 1 \le \alpha_1$, the group of FNNs (2.2) is said to be synchronization if there exist matrices $P_l > 0, \hat{\epsilon}_1 > 0, \hat{F}_{il}$, $G_l, \hat{H}_{il}, \hat{K}_{il}, \hat{M}_{il}, \hat{R}_s$, and $\hat{R}_{il}$ and scalars $\epsilon_2 > 0$ and $\epsilon_3 > 0$ such that Conditions (3.1), (3.3), and (4.1) hold for $\forall \sigma, l, j \in \Phi_l$.*

$$\begin{bmatrix} \hat{\Psi}_{11} & \overline{\mathcal{T}}_2\hat{\epsilon}_1 & \hat{\Psi}_{13} & \hat{\Psi}_{14} & 0 & \hat{\Psi}_{16} & 0 \\ * & -\hat{\epsilon}_1 & \hat{\Psi}_{23} & 0 & 0 & 0 & 0 \\ * & * & \hat{\Psi}_{33} & 0 & \hat{\Psi}_{35} & 0 & \hat{\Psi}_{37} \\ * & * & * & -\epsilon_2 I & 0 & 0 & 0 \\ * & * & * & * & -\epsilon_2 I & 0 & 0 \\ * & * & * & * & * & -\epsilon_3 I & 0 \\ * & * & * & * & * & * & -\epsilon_3 I \end{bmatrix} < 0, \tag{4.1}$$

where

$$\begin{aligned}
&\hat{\Psi}_{11} = -\alpha_2 P_l - \overline{\mathcal{T}}_1\hat{\epsilon}_1, \quad \hat{\Psi}_{23} = (I_{2N+1}\otimes B_l)^T\mathcal{G}_j^T,\\
&\hat{\mathcal{D}}_{222} = \mathrm{diag}_N\left\{\hat{D}_1, \hat{D}_2, \ldots, \hat{D}_N\right\},\\
&\hat{\Psi}_{13} = \hat{\mathcal{D}}_l j1^T + \left(\hat{\mathcal{M}}(\mathcal{L}\otimes I_{2m})C + \hat{\mathcal{K}}(\mathcal{L}\otimes I_{2n})\mathcal{I}\right)^T,\\
&\hat{\mathcal{D}}_l j1 = \begin{bmatrix} G_jD_l - \hat{R}_S C & 0 \\ \hat{\mathcal{R}} & \hat{\mathcal{D}}_{222} \end{bmatrix},\\
&\hat{\mathcal{R}}_{il} = \begin{bmatrix} 0 \\ \hat{R}_{il}C_l - \hat{R}_S C_l \end{bmatrix},\\
&\hat{D}_{ilj} = \begin{bmatrix} G_jD_l + \varsigma_i\hat{F}_{ij}C_l & \varsigma_i\hat{H}_{ij} \\ \hat{R}_{ij}C_l + \varsigma_i\hat{F}_{ij}C_l & GD_l - \hat{R}_iC_l + \varsigma_i\hat{H}_{ij} \end{bmatrix},\\
&\hat{\mathcal{R}} = \begin{bmatrix} \hat{\mathcal{R}}_{1l} & \hat{\mathcal{R}}_{2l} & \ldots & \hat{\mathcal{R}}_{Nl} \end{bmatrix}, \quad \hat{\mathcal{M}} = \begin{bmatrix} 0 & \hat{\mathcal{M}}_{12}^T \end{bmatrix}^T,\\
&\hat{\mathcal{M}}_{12} = \mathrm{diag}_N\left\{\hat{\mathcal{M}}_{121}, \hat{\mathcal{M}}_{122}, \ldots, \hat{\mathcal{M}}_{12N}\right\},\\
&\hat{\mathcal{K}}_{12} = \mathrm{diag}_N\left\{\hat{\mathcal{K}}_{121}, \hat{\mathcal{K}}_{122}, \ldots, \hat{\mathcal{K}}_{12N}\right\},\\
&\hat{\mathcal{M}}_{12i} = \begin{bmatrix} \hat{M}_{ij} & 0 \\ \hat{M}_{ij} & 0 \end{bmatrix}, \quad \hat{\mathcal{K}}_{12i} = \begin{bmatrix} 0 & \hat{K}_{ij} \\ 0 & \hat{K}_{ij} \end{bmatrix},\\
&\hat{\mathcal{K}} = \begin{bmatrix} 0 & \hat{\mathcal{K}}_{12}^T \end{bmatrix}^T, \quad \hat{\Psi}_{14} = \epsilon_2 C^T(N\otimes I_{2m})^T,\\
&\hat{\Psi}_{35} = \hat{\mathcal{M}}(M\otimes I_{2m}), \quad \hat{\Psi}_{16} = \epsilon_3\mathcal{I}^T(N\otimes I_{2n})^T,\\
&\hat{\Psi}_{37} = \hat{\mathcal{K}}(M\otimes I_{2n}), \quad \hat{\Psi}_{33} = P_\sigma - \mathcal{G}_j - \mathcal{G}_j^T,\\
&\mathcal{G}_j = \mathrm{diag}_{2N+1}\{G_j, G_j, \ldots, G_j\}.
\end{aligned}$$

Thus, the observer and controller gains are listed as follows:

$$\begin{aligned}
&F_{il} = G_l^{-1}\hat{F}_{il}, \quad H_{il} = G_l^{-1}\hat{H}_{il}, \quad K_{il} = G_l^{-1}\hat{K}_{il},\\
&M_{il} = G_l^{-1}\hat{M}_{il}, \quad R_{il} = G_l^{-1}\hat{R}_{il}, \quad R_s = G_l^{-1}\hat{R}_s.
\end{aligned}$$

Proof. In terms of the Schur complement theorem, the following inequality holds based on the condition (4.1):

$$\Sigma_1 + \epsilon_2\Sigma_2^T\Sigma_2 + \epsilon_2^{-1}\Sigma_3\Sigma_3^T + \epsilon_3\Sigma_4^T\Sigma_4 + \epsilon_3^{-1}\Sigma_5\Sigma_5^T < 0, \tag{4.2}$$

where

$$\begin{aligned}
&\Sigma_1 = \begin{bmatrix} -\alpha_2 P_l - \overline{\mathcal{T}}_1\hat{\epsilon}_1 & \overline{\mathcal{T}}_2\hat{\epsilon}_1 & \hat{\Psi}_{13} \\ * & -\hat{\epsilon}_1 & (I_{2N+1}\otimes B_l)^T\mathcal{G}_j^T \\ * & * & P_\sigma - \mathcal{G}_j - \mathcal{G}_j^T \end{bmatrix},\\
&\Sigma_2 = [(N\otimes I_{2m})C \quad 0 \quad 0],\\
&\Sigma_3 = \begin{bmatrix} 0 & 0 & (M\otimes I_{2m})^T\hat{\mathcal{M}}^T \end{bmatrix}^T,\\
&\Sigma_4 U = [(N\otimes I_{2n})\mathcal{I} \quad 0 \quad 0],\\
&\Sigma_5 = \begin{bmatrix} 0 & 0 & (M\otimes I_{2n})^T\hat{\mathcal{K}}^T \end{bmatrix}^T.
\end{aligned}$$

For every matrix $P_\sigma > 0$, we can get $P_\sigma^{-1} > 0$, and notice that $P_\sigma - \mathcal{G}_j$ is not a zero matrix. By the properties of positive definite matrices, we have

$$(P_\sigma - \mathcal{G}_j)P_\sigma^{-1}(P_\sigma - \mathcal{G}_j)^T \ge 0,$$

which implies

$$P_\sigma - \mathcal{G}_j - \mathcal{G}_j^T \ge \mathcal{G}_j P_\sigma^{-1}\mathcal{G}_j^T. \tag{4.3}$$

Define

$$\hat{F}_{il} \triangleq G_l F_{il}, \quad \hat{H}_{il} \triangleq G_l H_{il}, \quad \hat{K}_{il} \triangleq G_l K_{il},$$
$$\hat{M}_{il} \triangleq G_l M_{il}, \quad \hat{R}_{il} \triangleq G_l R_{il}, \quad \hat{R}_s \triangleq G_l R_s.$$

According to Lemma 2.1, (4.2), and (4.3), it follows that

$$\begin{bmatrix} -\alpha_2 P_l - \overline{\mathcal{T}}_1 \hat{\epsilon}_1 & \overline{\mathcal{T}}_2 \hat{\epsilon}_1 & \mathcal{D}^T \mathcal{G}_j^T \\ * & -\hat{\epsilon}_1 & (I_{2N+1} \otimes B_l)^T \mathcal{G}_j^T \\ * & * & -\mathcal{G}_j P_\sigma \mathcal{G}_j^T \end{bmatrix} < 0. \quad (4.4)$$

Pre-multiplying and post-multiplying the obtained inequality (4.4) with $\mathrm{diag}_3\left\{I, I, \mathcal{G}_j^{-1}\right\}$ and its transpose, the condition (3.2) holds, and the group of FNNs (2.2) will achieve synchronization by combining conditions (3.1) and (3.3). □

5. Illustrative example

To prove the validity of our results, we present a numerical example of FNNs (2.2) with five nodes here, whose parameters are as follows:

$$B_1 = \begin{bmatrix} -0.2 & -0.4 \\ -0.4 & -0.1 \end{bmatrix},$$
$$B_2 = \begin{bmatrix} 0.2 & -0.4 \\ -0.3 & -0.1 \end{bmatrix},$$
$$C_1 = \begin{bmatrix} 1 & 1 \end{bmatrix},$$
$$C_2 = \begin{bmatrix} 1 & 0 \end{bmatrix},$$
$$D_1 = \mathrm{diag}_2\{-0.85, -0.85\},$$
$$D_2 = \mathrm{diag}_2\{-0.85, -0.95\}.$$

According to the connection topology of DIOBC, as shown in Figure 1, its uncertain connection weights are expressed as

$$a_{12}(k) = a_{21}(k) = 0.8 + 0.1\sin(k),$$
$$a_{14}(k) = a_{41}(k) = 0.9 + 0.1\sin(k),$$
$$a_{23}(k) = a_{32}(k) = 1.1 + 0.1\sin(k),$$
$$a_{25}(k) = a_{52}(k) = 1 + 0.1\sin(k),$$
$$a_{34}(k) = a_{43}(k) = 1.2 + 0.1\sin(k),$$
$$a_{35}(k) = a_{53}(k) = 1 + 0.1\sin(k).$$

The pinning gains of the DIOBC are $\varsigma_1 = 1, \varsigma_2 = 1, \varsigma_3 = 0, \varsigma_4 = 1, \varsigma_5 = 0$.

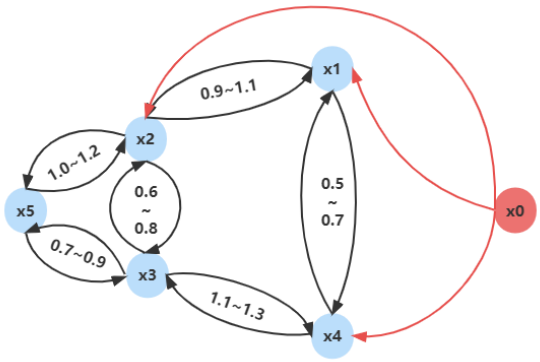

Figure 1. Impulsive signal of the DIOBC.

The nonlinear activation functions $g_i(\cdot), i \in \Phi_n$ of our discrete-time FNNs (2.2) are defined as

$$g_1(\boldsymbol{x}_{i1}(k)) = 0.2\left(|\boldsymbol{x}_{i1}(k) + 1| - |\boldsymbol{x}_{i1}(k) - 1|\right),$$
$$g_2(\boldsymbol{x}_{i2}(k)) = 0.1\left(|\boldsymbol{x}_{i2}(k) + 1| - |\boldsymbol{x}_{i2}(k) - 1|\right),$$

which imply $\underline{\vartheta}_1 = 0, \underline{\vartheta}_2 = 0, \bar{\vartheta}_1 = 0.4$ and $\bar{\vartheta}_2 = 0.2$.

Assuming that the iterative step side is $\varepsilon = 0.02$, according to the algorithm in [44], we can get that $\alpha_1 = 1.04, \alpha_2 = 0.76$, and the maximal allowed impulsive interval is $\tau = 8$. The observer and controller gains are listed below

$$R_0 = \begin{bmatrix} -0.1667 \\ -0.2082 \end{bmatrix}, \quad R_{11} = \begin{bmatrix} -0.1699 \\ -0.2081 \end{bmatrix},$$
$$R_{21} = \begin{bmatrix} -0.4254 \\ -0.5601 \end{bmatrix}, \quad R_{31} = \begin{bmatrix} -0.1411 \\ -0.1591 \end{bmatrix},$$
$$R_{41} = \begin{bmatrix} -0.2185 \\ -0.2761 \end{bmatrix}, \quad R_{51} = \begin{bmatrix} -0.1205 \\ -0.1325 \end{bmatrix},$$
$$H_{11} = \begin{bmatrix} 0.1318 & 0.0954 \\ 0.1360 & 0.1696 \end{bmatrix}, \quad F_{11} = \begin{bmatrix} 0.3010 \\ 0.3676 \end{bmatrix},$$
$$H_{21} = \begin{bmatrix} 0.0258 & -0.0589 \\ -0.0106 & -0.0628 \end{bmatrix}, \quad F_{21} = \begin{bmatrix} 0.4854 \\ 0.6181 \end{bmatrix},$$
$$H_{41} = \begin{bmatrix} 0.1570 & 0.1124 \\ 0.1769 & 0.1872 \end{bmatrix}, \quad F_{41} = \begin{bmatrix} 0.3744 \\ 0.4716 \end{bmatrix},$$
$$H_{31} = 0, \quad H_{51} = 0, \quad F_{31} = 0, \quad F_{51} = 0,$$
$$K_{11} = \begin{bmatrix} -0.0002 & -0.0005 \\ -0.0007 & -0.0009 \end{bmatrix}, \quad M_{11} = \begin{bmatrix} 0.0007 \\ 0.0003 \end{bmatrix},$$

$$K_{21} = \begin{bmatrix} 0.0152 & 0.0256 \\ 0.0203 & 0.0376 \end{bmatrix}, \quad M_{21} = \begin{bmatrix} -0.0321 \\ -0.0399 \end{bmatrix},$$

$$K_{31} = \begin{bmatrix} 0.0420 & 0.0284 \\ 0.0434 & 0.0453 \end{bmatrix}, \quad M_{31} = \begin{bmatrix} 0.0971 \\ 0.1133 \end{bmatrix},$$

$$K_{41} = \begin{bmatrix} -0.0150 & -0.0193 \\ -0.0212 & -0.0241 \end{bmatrix}, \quad M_{41} = \begin{bmatrix} -0.0188 \\ -0.0250 \end{bmatrix},$$

$$K_{51} = \begin{bmatrix} 0.0514 & 0.0348 \\ 0.0549 & 0.0531 \end{bmatrix}, \quad M_{51} = \begin{bmatrix} 0.1156 \\ 0.1297 \end{bmatrix},$$

$$R_{22} = \begin{bmatrix} -0.4254 \\ -0.6301 \end{bmatrix}, \quad R_{32} = \begin{bmatrix} -0.1351 \\ -0.1291 \end{bmatrix},$$

$$R_{42} = \begin{bmatrix} 0.2325 \\ -0.1224 \end{bmatrix}, \quad R_{52} = \begin{bmatrix} -0.1205 \\ -0.1435 \end{bmatrix},$$

$$H_{12} = \begin{bmatrix} 0.1423 & 0.1426 \\ 0.1356 & 0.1246 \end{bmatrix}, \quad F_{12} = \begin{bmatrix} 0.2430 \\ 0.5626 \end{bmatrix},$$

$$H_{22} = \begin{bmatrix} 0.0258 & -0.0589 \\ -0.2346 & -0.7428 \end{bmatrix}, \quad F_{22} = \begin{bmatrix} 0.4354 \\ 0.5381 \end{bmatrix},$$

$$H_{42} = \begin{bmatrix} 0.1570 & 0.1124 \\ 0.1419 & 0.4272 \end{bmatrix}, \quad F_{42} = \begin{bmatrix} 0.3454 \\ 0.1216 \end{bmatrix},$$

$$H_{32} = 0, \quad H_{52} = 0, \quad F_{32} = 0, \quad F_{52} = 0,$$

$$K_{12} = \begin{bmatrix} -0.0012 & -0.0004 \\ -0.0002 & -0.0010 \end{bmatrix}, \quad M_{12} = \begin{bmatrix} 0.0005 \\ 0.0007 \end{bmatrix},$$

$$K_{22} = \begin{bmatrix} 0.0152 & 0.0256 \\ 0.0352 & 0.0264 \end{bmatrix}, \quad M_{22} = \begin{bmatrix} -0.0523 \\ -0.0743 \end{bmatrix},$$

$$K_{32} = \begin{bmatrix} 0.0420 & 0.0284 \\ 0.0412 & 0.0653 \end{bmatrix}, \quad M_{32} = \begin{bmatrix} 0.0451 \\ 0.1112 \end{bmatrix},$$

$$K_{42} = \begin{bmatrix} -0.0150 & -0.0423 \\ -0.0412 & -0.0621 \end{bmatrix}, \quad M_{42} = \begin{bmatrix} -0.0588 \\ -0.0450 \end{bmatrix},$$

$$K_{52} = \begin{bmatrix} 0.0514 & 0.0348 \\ 0.0319 & 0.0521 \end{bmatrix}, \quad M_{52} = \begin{bmatrix} 0.3416 \\ 0.3256 \end{bmatrix},$$

$$R_{12} = \begin{bmatrix} -0.1252 \\ -0.3451 \end{bmatrix}.$$

The fuzzy rules membership functions are

$$\theta_1(k) = \sin^2(3k), \quad \theta_2(k) = \cos^2(3k).$$

The FNNs initial states are as follows:

$$\boldsymbol{s}(0) = \begin{bmatrix} 1 \\ -2 \end{bmatrix}, \quad \boldsymbol{x}_1(0) = \begin{bmatrix} 2 \\ 5 \end{bmatrix}, \quad \boldsymbol{x}_2(0) = \begin{bmatrix} -3 \\ 1 \end{bmatrix},$$

$$\boldsymbol{x}_3(0) = \begin{bmatrix} -1 \\ -2 \end{bmatrix}, \quad \boldsymbol{x}_4(0) = \begin{bmatrix} -4 \\ -3 \end{bmatrix}, \quad \boldsymbol{x}_5(0) = \begin{bmatrix} -2 \\ 4 \end{bmatrix},$$

Under the above conditions, the states of our three fuzzy neural nodes with impulsive control, general control, and without control are shown in Figures 2–4, respectively. We can see that in these three kinds, both impulsive control and general control will achieve synchronization along the expected trajectory over time, and the synchronization time is almost the same.

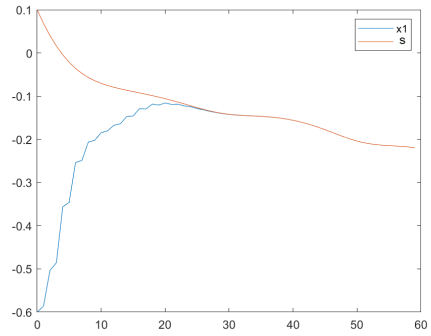

(a) with impulsive control

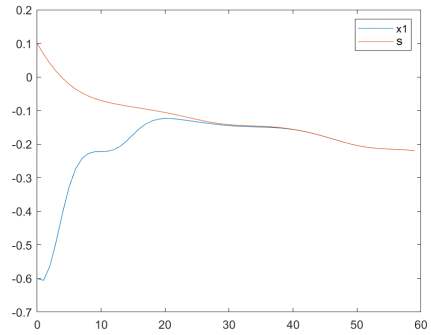

(b) with general control

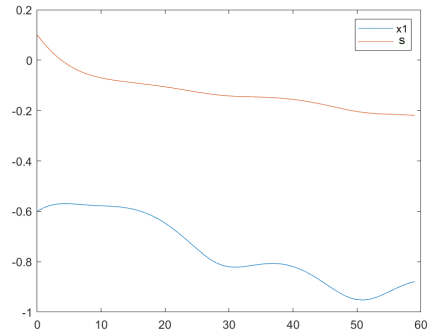

(c) without control

Figure 2. The state trajectories $x_1(k)$, $s(k)$ without and with the impulsive control.

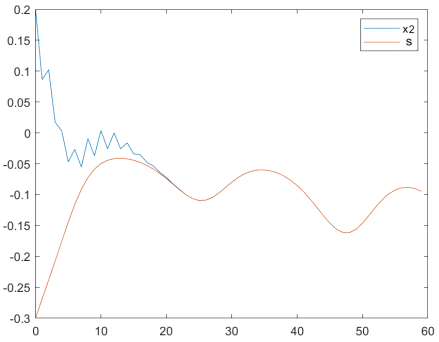

(a) with impulsive control

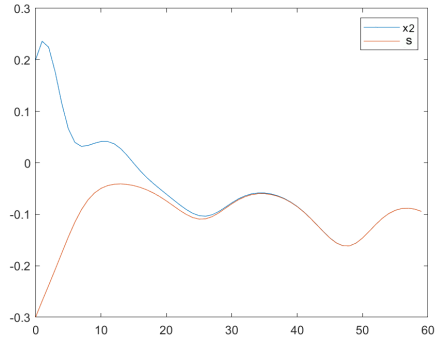

(b) with general control

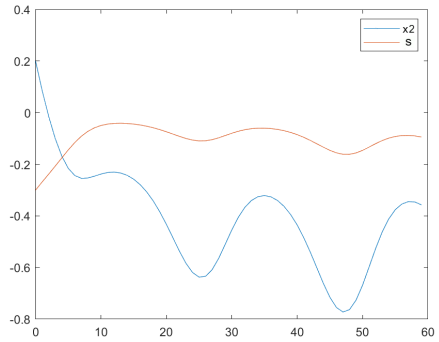

(c) without control

Figure 3. The state trajectories $x_2(k)$, $s(k)$ without and with the impulsive control.

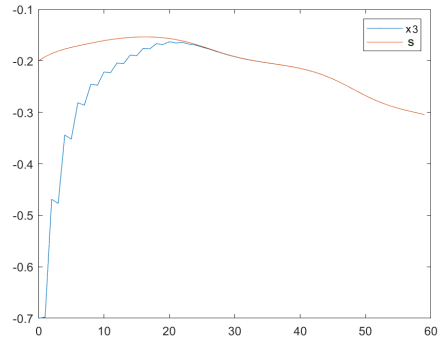

(a) with impulsive control

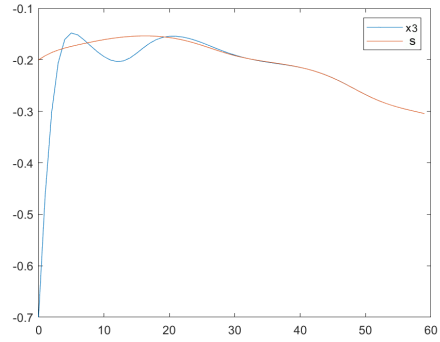

(b) with general control

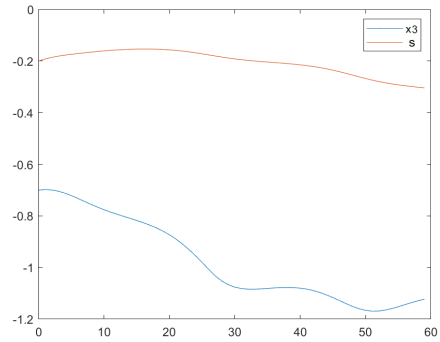

(c) without control

Figure 4. The state trajectories $x_3(k)$, $s(k)$ without and with the impulsive control.

However, as shown in Table 1, the control times of impulsive control to achieve synchronization are less than those of general control; that is, although the time required for impulsive control and general control to achieve synchronization is the same, the efficiency of impulsive control is higher than that of general control.

Table 1. Description of the model state variables.

Synchronization error	Impulsive control times	General control times
$\|e_1\| \leq 0.01$	16	27
$\|e_2\| \leq 0.01$	15	26
$\|e_3\| \leq 0.01$	19	27

6. Conclusions

In this paper, we investigate the synchronization property of a set of discrete-time FNNs, considering the case of uncertain information exchange caused by uncertain weights of nodes between FNNs nodes. Based on the measured partial states of FNNs, the controller based on the impulse observer is designed, the IAES is derived, and by proving the stability of IAES, the synchronization sufficient conditions of FNNs and the corresponding gain matrices of the observer and controller are obtained. Finally, a numerical example is given to illustrate the validity of our results.

Use of AI tools declaration

During the preparation of this work, we used the AI tool "QuillBot" in order to revise the grammar. After using this tool, we reviewed and edited the content as needed and take full responsibility for the content of the publication.

Acknowledgments

This work is supported by the National Natural Science Foundation of China Grant No. 12171065, the Science and Technology Research Program of Chongqing Municipal Education Commission Grant No. KJQN202000601, the Natrual Science Foundation Project of Chongqing under Grant cstc2020jcyj-msxmX0593, the Open Project of Key Laboratory No. CSSXKFKTM202007, Mathematical College, Chongqing Normal University.

Conflict of interest

All authors declare that they have no conflicts of interest.

References

1. J. Buckley, Y. Hayashi, Fuzzy neural networks: a survey, *Fuzzy Sets Syst.*, **66** (1994), 1–13. https://doi.org/10.1016/0165-0114(94)90297-6
2. X. Wang, Y. Yu, S. Zhong, K. Shi, N. Yang, D. Zhang, et al., Novel heterogeneous mode-dependent impulsive synchronization for piecewise T-S fuzzy probabilistic coupled delayed neural networks, *IEEE Trans. Fuzzy Syst.*, **30** (2021), 2142–2156. https://doi.org/10.1109/TFUZZ.2021.3076525
3. X. Wang, Y. Yu, K. Shi, H. Chen, S. Zhong, X. Yang, et al., Membership-mismatched impulsive exponential stabilization for fuzzy unconstrained multilayer neural networks with node-dependent delays, *IEEE Trans. Fuzzy Syst.*, **31** (2022), 1214–1228. https://doi.org/10.1109/TFUZZ.2022.3197925
4. X. Wang, Y. Yu, J. Cai, N. Yang, K. Shi, S. Zhong, et al., Multiple mismatched synchronization for coupled memristive neural networks with topology-based probability impulsive mechanism on time scales, *IEEE Trans. Cybern.*, **53** (2021), 1485–1498. https://doi.org/10.1109/TCYB.2021.3104345
5. A. Iwata, Y. Nagasaka, N. Suzumura, Data compression of the ECG using neural network for digital Holter monitor, *IEEE Eng. Med. Biol. Mag.*, **9** (1990), 53–57. https://doi.org/10.1109/51.59214
6. M. Patricia, D. Sánchez, Multi-objective optimization for modular granular neural networks applied to pattern recognition, *Inf. Sci.*, **460-461** (2018), 594–610. https://doi.org/10.1016/j.ins.2017.09.031
7. Y. Zhao, X. He, T. Huang, J. Huang, P. Li, A smoothing neural network for minimization l_1-l_p in sparse signal reconstruction with measurement noises, *Neural Networks*, **122** (2020), 40–53. https://doi.org/10.1016/j.neunet.2019.10.006
8. M. R. G. Meireles, P. E. Almeida, M. G. Simes, A comprehensive review for industrial applicability of artificial neural networks, *IEEE Trans. Ind. Electron.*, **50** (2003), 585–601. https://doi.org/10.1109/TIE.2003.812470

9. G. A. Carpenter, Neural network models for pattern recognition and associative memory, *Neural Networks*, **2** (1989), 243–257. https://doi.org/10.1016/0893-6080(89)90035-X
10. W. He, Y. Dong, Adaptive fuzzy neural network control for a constrained robot using impedance learning, *IEEE Trans. Neural Networks Learn. Syst.*, **29** (2017), 1174–1186. https://doi.org/10.1109/TNNLS.2017.2665581
11. Q. Song, W. Yu, J. Cao, F. Liu, Reaching synchronization in networked harmonic oscillators with outdated position data, *IEEE Trans. Cybern.*, **46** (2016), 1566–1578. https://doi.org/10.1109/TCYB.2015.2451651
12. T. Takagi, M. Sugeno, Fuzzy identification of systems and its applications to modeling and control, *IEEE Trans. Syst. Man Cybern.*, **15** (1993), 116–132. https://doi.org/10.1109/TSMC.1985.6313399
13. S. Selcuk, New stability results for Takagi-Sugeno fuzzy Cohen-Grossberg neural networks with multiple delays, *Neural Networks*, **114** (2019), 60–66. https://doi.org/10.1016/j.neunet.2019.02.010
14. A. Wu, Z. Zeng, Boundedness, Mittag-Leffler stability and asymptotical periodicity of fractional order fuzzy neural networks, *Neural Networks*, **74** (2016), 73–84. https://doi.org/10.1016/j.neunet.2015.11.003
15. Y. Xu, J. Li, R. Lu, C. Liu, Y. Wu, Finite-horizon l_2-l_∞ synchronization for time-varying Markovian jump neural networks under mixed-type attacks: observer-based case, *IEEE Trans. Neural Networks Learn. Syst.*, **30** (2018), 1695–1704. https://doi.org/10.1109/TNNLS.2018.2873163
16. X. Yang, G. Feng, C. He, J. Cao, Event-triggered dynamic output quantization control of switched T-S fuzzy systems with unstable modes, *IEEE Trans. Fuzzy Syst.*, **30** (2022), 4201–4210. https://doi.org/10.1109/TFUZZ.2022.3145808
17. J. Li, B. Zhang, R. Lu, Y. Xu, T. Huang, Distributed H_∞ state estimator design for time-delay periodic systems over scheduling sensor networks, *IEEE Trans. Cybern.*, **51** (2019), 462–472. https://doi.org/10.1109/TCYB.2019.2894392
18. Y. Xu, J. Dong, R. Lu, L. Xie, Stability of continuous-time positive switched linear systems: a weak common copositive Lyapunov functions approach, *Automatica*, **97** (2018), 278–285. https://doi.org/10.1016/j.automatica.2018.04.037
19. X. Xie, T. Wei, X. Li, Hybrid event-triggered approach for quasi-consensus of uncertain multi-agent systems with impulsive protocols, *IEEE Trans. Circuits Syst.*, **69** (2022), 872–883. https://doi.org/10.1109/TCSI.2021.3119065
20. H. Trentelman, K. Takaba, N. Monshizadeh, Robust synchronization of uncertain linear multi-agent systems, *IEEE Trans. Autom. Control*, **58** (2013), 1511–1523. https://doi.org/10.1109/TAC.2013.2239011
21. T. Li, M. Fu, L. Xie, J. Zhang, Distributed consensus with limited communication data rate, *IEEE Trans. Autom. Control*, **56** (2010), 279–292. https://doi.org/10.1109/TAC.2010.2052384
22. T. Li, F. Wu, J. Zhang, Multi-agent consensus with relative-state-dependent measurement noises, *IEEE Trans. Autom. Control*, **59** (2014), 2463–2468. https://doi.org/10.1109/TAC.2014.2304368
23. B. Liu, X. Liu, G. Chen, H. Wang, Robust impulsive synchronization of uncertain dynamical networks, *IEEE Trans. Circuits Syst. I*, **52** (2005), 1431–1441. https://doi.org/10.1109/TCSI.2005.851708
24. S. Yang, Z. Guo, J. Wang, Robust synchronization of multiple memristive neural networks with uncertain parameters via nonlinear coupling, *IEEE Trans. Syst. Man Cybern.*, **45** (2015), 1077–1086. https://doi.org/10.1109/TSMC.2014.2388199
25. T. Chen, X. Liu, W. Lu, Pinning complex networks by a single controller, *IEEE Trans. Circuits Syst. I*, **54** (2007), 1317–1326. https://doi.org/10.1109/TCSI.2007.895383
26. W. Yu, G. Chen, J. Lü, On pinning synchronization of complex dynamical networks, *Automatica*, **45** (2009), 429–435. https://doi.org/10.1016/j.automatica.2008.07.016
27. X. Li, X. Yang, S. Song, Lyapunov conditions for finite-time stability of time-varying time-delay systems, *Automatica*, **103** (2019), 135–140. https://doi.org/10.1016/j.automatica.2019.01.031
28. X. Yang, Y. Liu, J. Cao, L. Rutkowski, Synchronization of coupled time-delay neural networks with mode-dependent average dwell time switching, *IEEE Trans. Neural Networks Learn. Syst.*, **31** (2020), 5483–5496. https://doi.org/10.1109/TNNLS.2020.2968342

29. J. Lu, C. Ding, J. Lou, J. Cao, Outer synchronization of partially coupled dynamical networks via pinning impulsive controllers, *J. Franklin Inst.*, **352** (2015), 5024–5041. https://doi.org/10.1016/j.jfranklin.2015.08.016

30. X. Li, S. Song, J. Wu, Exponential stability of nonlinear systems with delayed impulses and applications, *IEEE Trans. Automa. Control*, **64** (2019), 4024–4034. https://doi.org/10.1109/TAC.2019.2905271

31. X. Li, D. Ho, J. Cao, Finite-time stability and settling-time estimation of nonlinear impulsive systems, *Automatica*, **99** (2019), 361–368. https://doi.org/10.1016/j.automatica.2018.10.024

32. X. Li, X. Yang, J. Cao, Event-triggered impulsive control for nonlinear delay systems, *Automatica*, **117** (2020), 108981. https://doi.org/10.1016/j.automatica.2020.108981

33. X. Li, D. Peng, J. Cao, Lyapunov stability for impulsive systems via event-triggered impulsive control, *IEEE Trans. Autom. Control*, **65** (2020), 4908–4913. https://doi.org/10.1109/TAC.2020.2964558

34. W. Zhu, D. Wang, L. Liu, G. Feng, Event-based impulsive control of continuous-time dynamic systems and its application to synchronization of Memristive neural networks, *IEEE Trans. Neural Networks Learn. Syst.*, **29** (2018), 3599–3609. https://doi.org/10.1109/TNNLS.2017.2731865

35. S. Ding, Z. Wang, Event-triggered synchronization of discrete-time neural networks: a switching approach, *Neural Networks*, **125** (2020), 31–40. https://doi.org/10.1016/j.neunet.2020.01.024

36. H. Rao, F. Liu, H. Peng, Y. Xu, R. Lu, Observer-based impulsive synchronization for neural networks with uncertain exchanging information, *IEEE Trans. Neural Networks Learn. Syst.*, **31** (2020), 3777–3787. https://doi.org/10.1109/TNNLS.2019.2946151

37. P. Chen, J. Wang, S. He, X. Luan, F. Liu, Observer-based asynchronous fault detection for conic-type nonlinear jumping systems and its application to separately excited DC motor, *IEEE Trans. Circuits Syst. I*, **67** (2019), 951–962. https://doi.org/10.1109/TCSI.2019.2949368

38. M. de Magistris, M. di Bernardo, E. di Tucci, S. Manfredi, Synchronization of networks of non-identical Chua's circuits: analysis and experiments, *IEEE Trans. Circuits Syst. I*, **59** (2012), 1029–1041. https://doi.org/10.1109/TCSI.2012.2185279

39. F. Liu, C. Liu, R. Rao, Y. Xu, T. Wang, Reliable impulsive synchronization for fuzzy neural networks with mixed controllers, *Neural Networks*, **143** (2021), 759–766. https://doi.org/10.1016/j.neunet.2021.08.013

40. P. Chen, S. He, V. Stojanovic, X. Luan, F. Liu, Fuzzy fault detection for Markov jump systems with partly accessible hidden information: an event-triggered approach, *IEEE Trans. Cybern.*, **52** (2021), 7352–7361. https://doi.org/10.1109/TCYB.2021.3050209

41. H. Rao, F. Liu, H. Peng, Y. Xu, R. Lu, Observer-based impulsive synchronization for neural networks with uncertain exchanging information, *IEEE Trans. Neural Networks Learn. Syst.*, **31** (2020), 3777–3787. https://doi.org/10.1109/TNNLS.2019.2946151

42. L. Wang, Z. Wang, Q. Han, G. Wei, Synchronization control for a class of discrete-time dynamical networks with packet dropouts: a coding-decoding-based approach, *IEEE Trans. Cybern.*, **48** (2018), 2437–2448. https://doi.org/10.1109/TCYB.2017.2740309

43. L. Xie, Output feedback H_∞ control of systems with parameter uncertainty, *Int. J. Control*, **63** (1996), 741–750. https://doi.org/10.1080/00207179608921866

44. H. Rao, F. Liu, H. Peng, Y. Xu, R. Lu, Observer-based impulsive synchronization for neural networks with uncertain exchanging information, *IEEE Trans. Neural Networks Learn. Syst.*, **31** (2020), 3777–3787. https://doi.org/10.1109/TNNLS.2019.2946151

AIMS Press